

Sub-microscopic transient lens spectroscopy of InGaN/GaN quantum wells

Koichi Okamoto^{*,1}, Shigeo Fujita², Yoichi Kawakami², and Axel Scherer¹

¹ Department of Electrical Engineering, California Institute of Technology, Pasadena, CA 91125, USA

² Department of Electronic Science and Engineering, Kyoto University, Kyoto 606-8501, Japan

Received 11 April 2003, revised 1 August 2003, accepted 5 August 2003

Published online 15 October 2003

PACS 68.37.Uv, 72.20.Jv, 73.63.Hs, 78.67.De

Transient lens (TL) spectroscopy was developed with sub-micrometer spatial resolution to observe the temporal and special behavior of the nonradiative processes of carrier dynamics in InGaN/GaN quantum wells (QW). We have observed the carrier density dynamics and the thermal dynamics in the TL signals with a nanosecond pulsed laser. We have also observed TL and photoluminescence (PL) signals by using near-field scanning optical microscopy (NSOM), and find that both PL and TL images are correlated and exhibit submicron scale spatial inhomogeneity.

© 2003 WILEY-VCH Verlag GmbH & Co. KGaA, Weinheim

1 Introduction Currently, InGaN/GaN based quantum well (QW) optical devices (light emitting diodes; LED and laser diode; LD) have been studied and developed for a wide range of applications. Recently, we have reported on the temporal and spatial resolved observation of the radiative processes in InGaN/GaN-based QW probed by time-resolved micro-photoluminescence (TRMPL) [1] and scanning near-field optical microscopy (NSOM) [2]. We have also succeeded in the direct observation of the non-radiative processes (thermalization, heat conduction [3] and carrier diffusion [4]) by using transient grating (TG) spectroscopy. Although nonradiative processes of carriers are very important in determining optical emission properties, only few investigations have so far been conducted to experimentally elucidate the nonradiative processes, primarily due to the difficult nature of such measurements. We expect that transient lens (TL) spectroscopy, which has been developed for the photochemistry research field [5, 6], is also applicable for the direct observation of nonradiative carrier processes. The principle of TL spectroscopy, which is based on the third order nonlinear optical effect, is similar to TG spectroscopy, but the experimental configuration is much simpler and the spatial resolution is significantly improved. Recently, we have reported for the first time an investigation of the TL spectroscopy to experimentally observe nonradiative processes in GaN and InGaN/GaN materials [7]. In this work, we show results from TL spectroscopy measurements with micro or sub-micro spatial resolution, and observe the temporal and special behavior of nonradiative processes of carries in InGaN/GaN quantum wells.

2 Experimental The experimental setup of the time-resolved TL technique (TR-TL) with microscopic resolution has been described in detail elsewhere [7]. A frequency-tripled Nd:YAG laser (355 nm) and a cw-He-Ne laser (633 nm) were used as pump and probe beams, respectively. The pulse width, power and repetition rate of the pump beam are 10 ns, 0.3 mJ/pulse and 3 Hz, respectively. Both pump and probe beams were focused by an objective lens (X40) on the sample. Focusing or defocusing of the probe beam by the transient lens effect, which is created by the photoinduced refractive index change (Δn), was detected with a pinhole, a glass filter, and a photomultiplier.

* Corresponding author: e-mail: kokamoto@caltech.edu, Phone: +1 626 395 2206, Fax: +1 626 683 9547

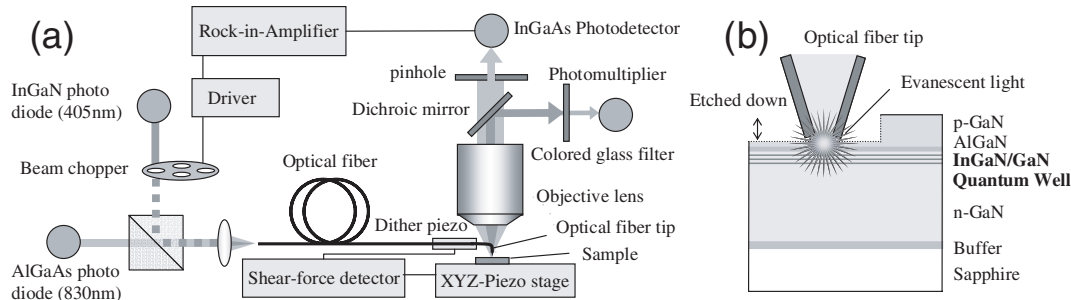


Fig. 1 a) Experimental setup for the transient lens (TL) spectroscopy with the near-field scanning optical microscope (NSOM). b) Sample structure of the InGaN/AlGaN/GaN LED wafer.

A schematic diagram describing the near-field scanning measurement using the TL method (NSOM-TL) with sub-microscopic resolution is shown in Fig. 1a. Quite recently, Fujinami et al. [8] reported a photo-thermal near-field scanning optical microscope based on the thermal lens technique. Our experimental setup is similar, and we used a Twin-SNOM system manufactured by OMICRON with a time-modulated (400 Hz) InGaN laser (405 nm) and a cw-AlGaAs laser (830 nm) as pump and probe beams, respectively. Both beams were coupled into a metal-coated optical fiber tip. The aperture size at the end of the tip was 200 nm, and the pump and probe beam power levels, before coupling into the optical fiber, were 5 mW and 1 mW respectively. The photoluminescence (PL) signal and the TL signal were separated by using a dichroic mirror and colored glass filter and detected with a photomultiplier and a highly sensitive (fW) InGaAs photodiode with a lock-in amplifier system, respectively. The fiber tip is positioned at the dither piezo device and shear-force detector in order to control the distance between the tip and the sample surface (≈ 10 nm) and to obtain a topographic image of the sample. The sample stage was scanned in an x - y direction by a piezo actuator. All of the measurements were performed at room temperature.

The InGaN/GaN/AlGaN-based LED wafer with green emission (525 nm), grown by a metal-organic chemical vapor deposition (MOCVD) on sapphire substrate, was purchased from AXT Inc. In order to reduce the distance between the optical fiber tip and the active layer and move the quantum well further into the evanescent light field, we etched the upper layer of the sample surface by using chemically assisted ion beam etching (CAIBE) with Xe and Cl_2 gases. The geometry and process parameters used for the etching process were similar to those provided in Ref. [9]. The thickness of the upper layer after etching was less than 100 nm. The sample structure and the configuration of the sample surface and the optical fiber tip were shown in Fig. 1b.

3 Results and discussions Figure 2a shows the time profiles of the TR-TL signals with 3 μm and 100 μm spot sizes at room temperature. The measured TL signals have two components; a spike-like positive ($\Delta n > 0$) component and a slowly-decaying negative ($\Delta n < 0$) component. From the relationship of $(\partial n / \partial N) > 0$ [10] and $(\partial n / \partial T) < 0$ [11] in GaN, we assigned the fast component and slow component to the convex lens effect of the carrier density change (ΔN) and the concave lens effect of the temperature change (ΔT), respectively. The signal intensities and decay times of the fast components represent the light-generated carrier density and the carrier recombination/diffusion processes, respectively. On the other hand, the signal intensities and decay rates of the slow components represent the amount of the thermal energy released by the nonradiative recombination of carriers (thermalization) and the heat conduction, respectively. By solving the rate equations of carrier and heat dynamics, the decay lifetimes of the carrier density (τ_c) and thermal (τ_{th}) components in the TL signals are given by

$$\frac{1}{\tau_c} = \frac{4D}{w_0^2} + \frac{1}{\tau_{\text{rad}}} + \frac{1}{\tau_{\text{non-rad}}}, \quad (1a)$$

$$\frac{1}{\tau_{\text{th}}} = \frac{4\kappa}{\rho C_p w_0^2} \quad (1b)$$

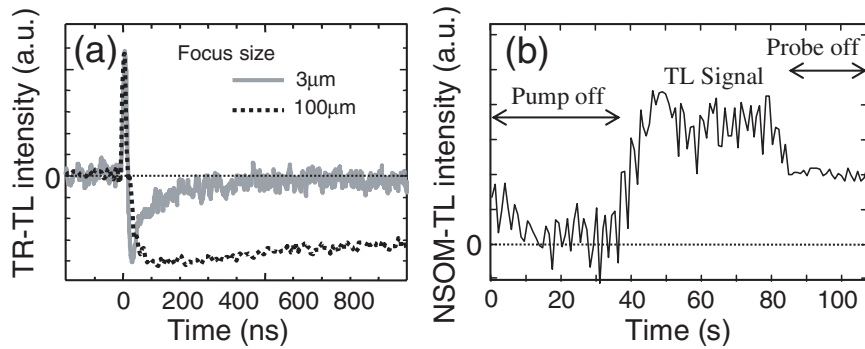


Fig. 2 Time profiles of the a) TR-TL signals with the nanosecond pulsed laser and b) NSOM-TL signals taken for the InGaN/GaN.

where w_0 , D , τ_{rad} , $\tau_{\text{non-rad}}$, κ , ρ , and C_p are the focus size, carrier diffusivity, radiative, nonradiative recombination lifetime, heat conductivity, density, and the heat capacity, respectively [7]. These parameters can be obtained by the fitting and analysis of the time profiles of the TL signals.

Figure 2b shows the raw signal of the NSOM-TL measurement of the InGaN/GaN QW. We used an integration time for the lock-in measurement of 1 second. The S/N ratio of this signal was low but the NSOM-TL signal could be confirmed by comparing the signal intensities with pump-off and probe-off measurements.

Figure 3 shows the obtained images of (a) topography, (b) reflection, (c) PL and (d) TL signals of the InGaN/GaN. The dark spots in the topographic and refractive images are etch-pits created on the sample surface by the dry etching process. Except for the etch-pits, both topographic and reflective images seemed almost homogeneous. On the other hand, we found a sub-micron scale spatial inhomogeneity in the near-field image of both PL and TL signals. Spatial inhomogeneities of PL intensities and peak wavelengths in InGaN/GaN QWs were previously reported by cathodoluminescence (CL) [12–14] and NSOM [2, 15] measurements and interpreted to be a result of fluctuations of the indium composition, the QW thickness, and the piezoelectric field in InGaN active layers. These fluctuations are very important and may act as the carrier localization centers, and suppress the pathways for nonradiative recombination of carriers. Such carrier localization has been known as one of the reasons for the strong emission properties in InGaN/GaN materials.

In this study, we found that the NSOM-TL image was also distributed inhomogeneously on a sub-micron scale. This suggests that the nonradiative carrier processes (diffusion, localization, or thermalization) should also be spatially distributed at submicron scales. We also found a strong correlation between the PL and the TL images. Areas with high TL signal intensity are expected to correspond to areas with the following properties; (1) high carrier density, (2) low carrier diffusivity, (3) low thermalization, or (4)

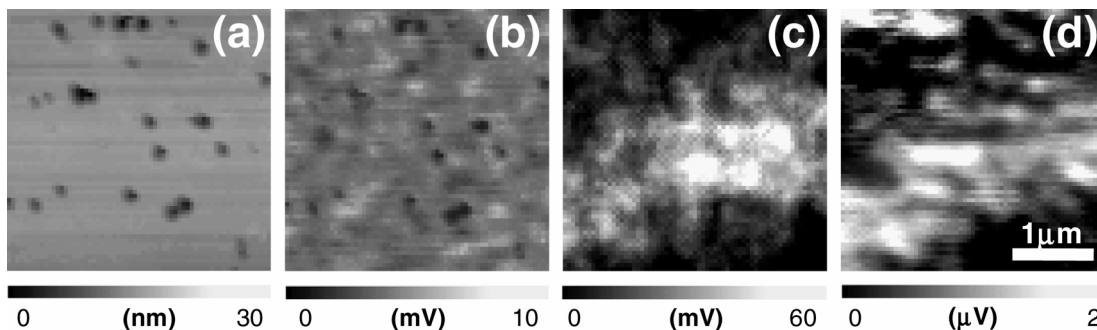


Fig. 3 a) Shear force topographic image, b) reflective light image, c) photoluminescence (PL) image, and d) transient lens (TL) images with the near-field measurement taken for the InGaN/GaN.

high thermal conductivity. The decay lifetime of the carrier density signal was calculated by the Eq. (1b) with $w_0 = 200$ nm and $D = 0.5$ cm²s⁻¹ [3]. The carrier diffusion time ($w_0^2/4D = 200$ ps) is much faster than the carrier recombination lifetime (τ_{rad} and $\tau_{\text{non-rad}}$) because the measured PL lifetime (τ_{PL} ; $1/\tau_{\text{PL}} = 1/\tau_{\text{rad}} + 1/\tau_{\text{non-rad}}$) was of the order of a few nanoseconds. Under this condition, the carrier density signal represents the main component in the NSOM-TL signal and the thermal signal may be negligible. Therefore, the TL images can be used to represent the carrier density in active layers and the bright region should correspond to the carrier localization areas. By comparing Figs. 3c with 3d, it was found that the many bright regions in the TL images correspond to the bright regions in the PL images. In these regions, carrier localized areas are well act as the radiative recombination (emission) centers. On the other hand, some bright TL regions correspond to the dark region in the PL image. We believe that these regions should be represented to the nonradiative recombination (thermalization) centers of carriers in the materials. To the best of our knowledge, this is the first report of the direct mapping of the distribution of the carrier density and the nonradiative recombination in InGaN/GaN-based optical devices.

4 Conclusions Temporal and spatially resolved TL spectroscopy is a powerful technique to observe the nonradiative carrier dynamics (diffusion, localization, thermalization, and heat conduction) in semiconductor materials. We found that the near-field TL images of InGaN/GaN exhibit sub-microscopic inhomogeneities, which we attribute to radiative and nonradiative recombination centers in the semiconductor quantum well structure.

Acknowledgements The authors would like to thank Prof. Masahide Terazima (Kyoto University) for valuable suggestions and discussions. A part of this study was supported by the Japan Society for the Promotion of Science (No. 12002454), and Caltech MURI Center for Quantum Networks, DARPA (MDA 972-00-1-0019), and AFOSR (F49620-01-6-0497).

References

- [1] T. Izumi, Y. Narukawa, K. Okamoto, Y. Kawakami, Shigeo Fujita, and S. Nakamura, *J. Lumin.* **87**, 1196 (2000).
- [2] A. Kaneta, K. Okamoto, Y. Kawakami, Sg. Fujita, G. Marutsuki, Y. Narukawa, and T. Mukai, *Appl. Phys. Lett.* **81**, 4353 (2002).
- [3] K. Okamoto, Y. Kawakami, Shigeo Fujita, and M. Terazima, *Analyt. Sci.* **17**, s312 (2001).
- [4] K. Okamoto, A. Kaneta, K. Inoue, Y. Kawakami, M. Terazima, T. Mukai, G. Shinomiya, and Sg. Fujita, *phys. stat. sol. (b)* **228**, 81 (2001).
- [5] M. Terazima, *Chem. Phys. Lett.* **230**, 87 (1994).
- [6] M. Terazima, T. Hara, and N. Hirota, *J. Phys. Chem.* **97**, 10554 (1993).
- [7] K. Okamoto, K. Inoue, Y. Kawakami, Sg. Fujita, M. Terazima, A. Tsujimura, and I. Kidoguchi, *Rev. Sci. Instrum.* **74**, 575 (2003).
- [8] M. Fujinami, K. Toya, and T. Sawada, *Rev. Sci. Instrum.* **74**, 621 (2003).
- [9] T. Yoshie, C. Cheng, and A. Scherer, *Proc. of IEEE International Semiconductor Laser Conference* 189 (1998).
- [10] H. Haag, B. Hönerlage, O. Briot, and R. L. Aulombard, *Phys. Rev. B* **60**, 11624, (1999).
- [11] L. Siozade, S. Colard, M. Mihailovic, J. Leymarie, A. Vasson, N. Grandjean, M. Leroux, and J. Massies, *Jpn. J. Appl. Phys.* **39**, 20, (2000).
- [12] T. Sugahara, M. Hao, T. Wang, D. Nakagawa, Y. Naoi, K. Nishino, and S. Sakai, *Jpn. J. Appl. Phys.* **37**, L1195 (1998).
- [13] S. Chichibu, K. Wada, and S. Nakamura, *Appl. Phys. Lett.* **71**, 2346 (1997).
- [14] F. Bertram, S. Srinivasan, L. Geng, F. A. Ponce, T. Riemann, and J. Christen, *Appl. Phys. Lett.* **80**, 3524 (2002).
- [15] D. K. Young, M. P. Mack, A. C. Abare, M. Hansen, L.A. Coldren, S. P. Denbaars, E. L. Hu, and D. Awschalom, *Appl. Phys. Lett.* **74**, 2349 (1999).